I&EC research
Industrial & Engineering Chemistry Research
pubs.acs.org/IECR
Article

Numerical Short-Cut Design of Simulated Moving Bed Chromatography for Multicomponent Nonlinear Adsorption Isotherms: Nonstoichiometric Langmuir Model

Ju Weon Lee,* Achim Kienle, and Andreas Seidel-Morgenstern

Cite This: *Ind. Eng. Chem. Res.* 2021, 60, 10753−10763

Read Online

ACCESS | Metrics & More | Article Recommendations | Supporting Information

ABSTRACT: For the fine chemical and pharmaceutical industries, simulated moving bed (SMB) chromatography is a very promising separation process. Because of its structural and operational complexity this periodically operated multicolumn process is not easy to design and optimize. In the 1990s, Storti, Mazzotti, and Morbidelli exploited the potential of the equilibrium theory and developed a now well-established short-cut design method for the conventional four-zone SMB processes. The concept, which is known as the "triangle theory", provides explicit design rules for a small set of nonlinear adsorption isotherm models and the case of processing binary feed mixtures. For the sake of extending the triangle theory to multicomponent systems, we introduce in this work a numerical short-cut method. The iterative method will be illustrated to design a conventional four-zone SMB process for the separation of quaternary mixtures obeying nonstoichiometric Langmuir isotherms. The results will be validated by comparing predicted internal concentration profiles with the results of additionally carried out true moving bed simulations.

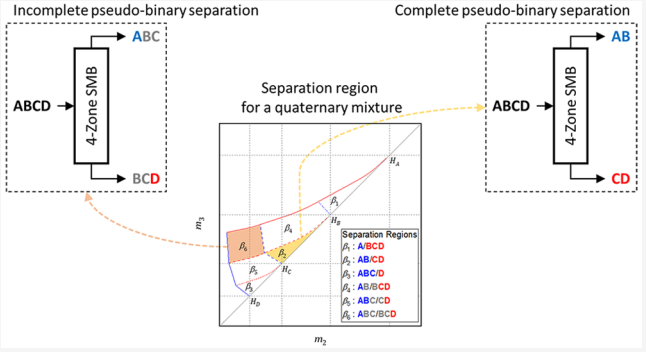

1. INTRODUCTION

In preparative chromatography, the application of classical batch elution is still the prevailing technology. Several more complicated modes of operation were developed in order to overcome the limitations of batch chromatography with respect to productivity, recovery, and solvent economy.[1] Among these modes the periodically operated multicolumn simulated moving bed (SMB) process is particularly productive.

The SMB process was suggested in 1961 by Universal Oil Products (UOP).[2] The various types of SORBEX processes were the first successful large-scale applications to separate the components of the "C8-Cut" of the steam cracker.[3] Dedicated arrangements of several columns are also used in the sugar industry for separating glucose and fructose.[4] In the last years, triggered by the first successful continuous chiral separation,[5] the concept has found numerous applications in the pharmaceutical industry, in particular for the separation of enantiomers.[6] SMB chromatography has often proven to lead to higher productivities and lower solvent consumptions compared to batch chromatography.[7,8]

To introduce the SMB process, it is instructive to consider first a hypothetical true moving bed (TMB) process. Classical four-zone countercurrent chromatography is illustrated schematically in Figure 1a. The hypothetical process assumes that there is a real countercurrent motion between the fluid phase (a gas, a liquid, or a supercritical fluid) and the solid phase. The TMB process is characterized by two streams entering the unit: the feed stream containing the mixture to be separated and the desorbent or eluent stream. The conventional process acts as a binary fractionator and can separate feed mixtures consisting of two components. For suitable operating conditions, one of the outgoing streams is enriched with the less-retained component (stars in Figure 1; the raffinate stream) and the other with the more-retained component (diamonds in Figure 1; the extract stream). The four streams divide the unit into four zones, each of which has to perform specific tasks. The separation of the two feed components should happen in the two central zones 2 and 3. Here, the net flow rates need to be set so that the less-retained component is carried in the direction of the raffinate outlet and the more-retained component in the direction of the extract outlet. The desorbent is fed to zone 1 in order to desorb the more-retained component and, thus, to regenerate the solid phase. The less-retained component is adsorbed onto the solid phase in zone 4 in order to regenerate the desorbent.

Special Issue: Giuseppe Storti Festschrift

Received: February 15, 2021
Revised: April 24, 2021
Accepted: April 27, 2021
Published: May 27, 2021

https://doi.org/10.1021/acs.iecr.1c00671
Ind. Eng. Chem. Res. 2021, 60, 10753−10763

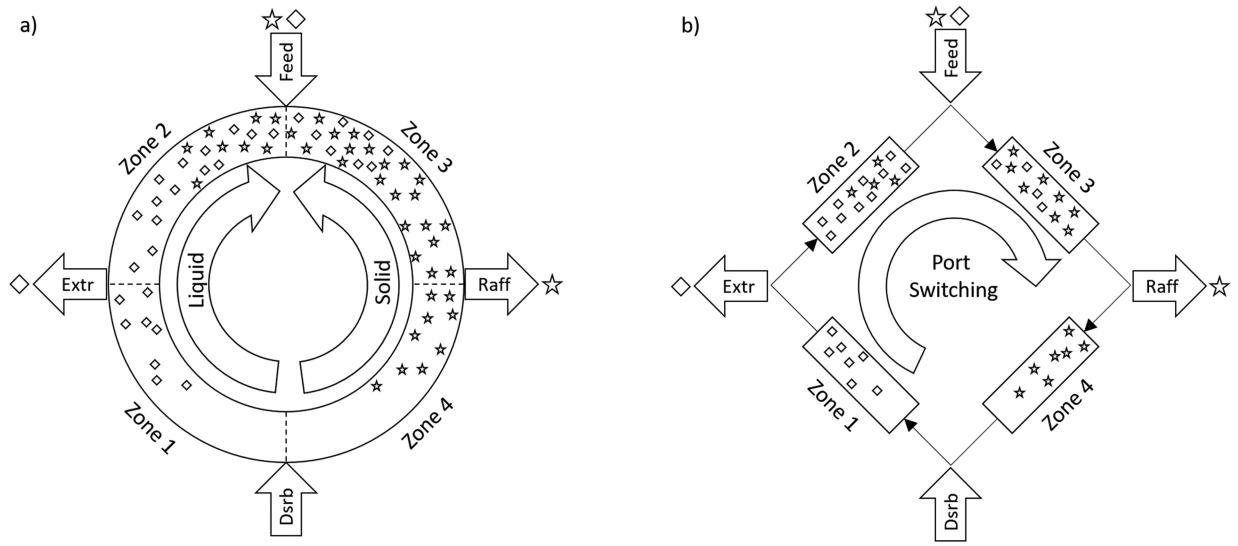

Figure 1. Schematic illustrations of (a) four-zone true moving bed and (b) four-zone simulated moving bed: Extr, extract port; Raff, raffinate port; Dsrb, desorbent port. The stars (☆) represent the less-retained component and the diamonds (◇) represent the more-retained component.

In the ideal TMB process, the solid (adsorbent) and the liquid (desorbent) phases move in a continuous manner counter-currently as plug flows (Figure 1a). Because of practical difficulties to realize such counter-current plug-flows, the solid phase flow is simulated by periodically switching the positions of the inlet and outlet ports (Figure 1b). However, the simple description of the hypothetical TMB process not only is helpful to explain the general principle of the implemented SMB process, it also supports designing the SMB process, in particular to specify the most relevant operating parameters. The success of SMB chromatography and its wider use was indeed supported strongly by the application of the equilibrium theory to identify suitable regions for the internal flows in the four zones and the switching time. The elegant theory, which neglects kinetic effects causing band broadening was introduced in depth.[9−12]

Equilibrium theory was applied to analyze a series connection of several columns in seminal papers by Storti, Mazotti, and Morbidelli. In particular instructive are the papers,[13−15] through which practitioners can become familiar with the key principle capable of deriving equations for the borders of the separation region. Through the application of equilibrium theory to the columns in the TMB unit and exploitation of the equivalence between the SMB and the TMB process, a set of user-friendly design criteria has been developed for binary mixture separation problems if the equilibria can be described by competitive Langmuir adsorption isotherms. Solutions for a very flexible extension to a generalized Langmuir isotherm model are also available.[16] More recently Fechtner and Kienle discussed equilibrium theory for stoichiometric ion exchange with an implicit sorption isotherm[17] and extended triangle theory to ion exchange SMB processes.[18]

The main outcome of the analysis based on the equilibrium theory is the identification of regions for dimensionless flow-rate ratios in the four zones. In particular, the specification of suitable flow-rates in the two separation zones 2 and 3 is most relevant. For linear adsorption isotherms, the region of exploitable flow-rates is a triangle in the "m_2−m_3 plane" bounded by the two adsorption equilibrium constants. This shape explains the well-established name for the "triangle theory" frequently used for designing SMB processes. The triangle theory provides an elegant framework that supports the understanding of SMB process operation and the development of specific and more advanced new SMB variants. As stated,[12] its importance and role in facilitating the widespread use of the SMB technology at all scales from the lab to production cannot be underestimated.

Summarizing the above, for binary separation problems obeying simple nonlinear isotherms, essential flow-rate requirements can be explicitly expressed.[13−16] However, there are more than two components that need to be separated in many practical cases. Moreover, more complex adsorption isotherm models are needed to accurately describe the underlying equilibria (e.g., implicit isotherm equations originating from the ideal adsorbed solution theory, IAST[19]). In such cases, it is not possible to identify analytically explicit values for the flow-rate borders of the exploitable separation regions, and thus, optimal operating conditions are typically determined exploiting time-consuming numerical scanning techniques.

In this work, we will introduce a novel iterative numerical method that extends the applicability of the well-established and very illustrative triangle theory to feed mixtures containing more than two components, which are characterized by a Langmuir type of adsorption isotherms. The identification of optimal operating conditions will be illustrated for splitting a quaternary feed mixture into two pseudo-components using a conventional four-zone SMB process. To treat often encountered cases, the adsorption isotherms of the four components considered are described by competitive Langmuir isotherms possessing component-dependent saturation capacities (non-stoichiometric isotherms).

2. THEORY

To determine the feasible operating conditions of the four-zone SMB process, the directions of the component migrations that can be determined by the partition coefficient of the component and the flow-rate ratio of the liquid phase to the solid phase in the zones should be properly assigned. Dimensionless m-values are defined as[14]

https://doi.org/10.1021/acs.iecr.1c00671
Ind. Eng. Chem. Res. 2021, 60, 10753−10763

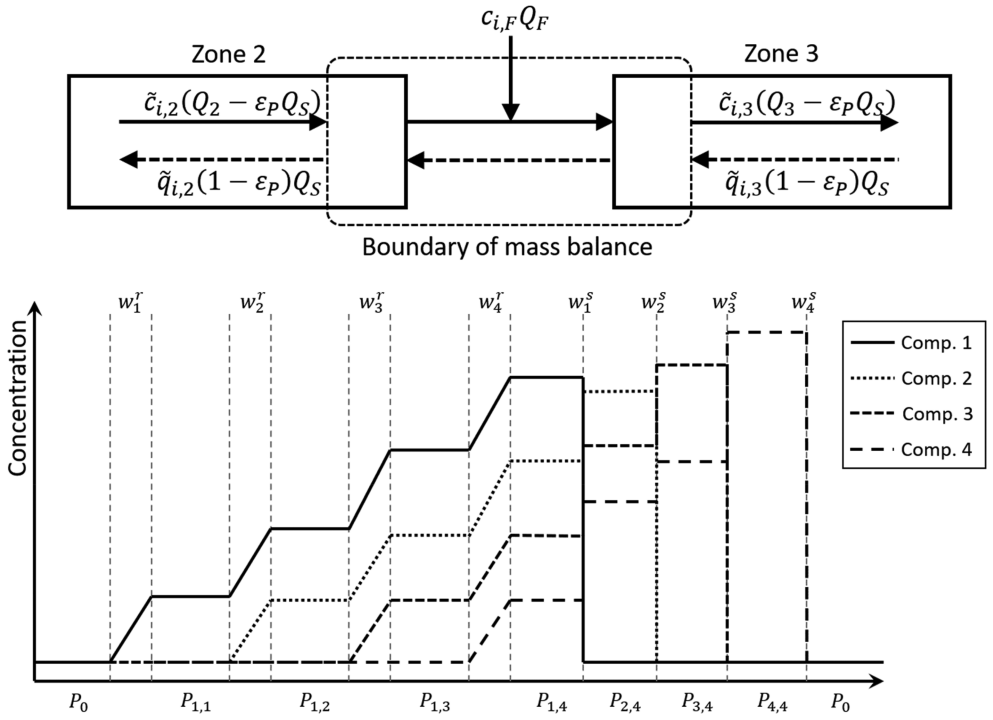

Figure 2. Schematic illustrations of mass balance around the feed port (upper) and the corresponding internal concentration plateau chart (lower) for quaternary mixture system. Solid arrows, liquid flows; dashed arrows, solid flows; Comp. 1 to 4, quaternary mixture components; P_0, base plateau; all component concentrations are zero; $P_{i,j}$, plateau in which the components i to j are not zero.

$$m_j = \frac{Q_j^{\mathrm{TMB}} - \varepsilon_P Q_s^{\mathrm{TMB}}}{(1-\varepsilon_P)Q_s^{\mathrm{TMB}}} = \frac{Q_s^{\mathrm{SMB}} - \varepsilon_T V_C^{\mathrm{SMB}}/t_S^{\mathrm{SMB}}}{(1-\varepsilon_T)V_C^{\mathrm{SMB}}/t_S^{\mathrm{SMB}}}$$
$$\text{s. t. } j \in \{1, 2, 3, 4\} \quad (1)$$

where the four m_j is the flow-rate ratio of the liquid phase to the solid phase in zone j, Q_j is the volumetric flow-rate of the liquid phase in zone j, ε_I is the interparticle void fraction, ε_P is the intraparticle void fraction, ε_T is the total void fraction ($= \varepsilon_I + (1 - \varepsilon_I)\varepsilon_P$), Q_S is the volumetric flow-rate of the solid phase, V_C is the empty column volume, t_S is the port switching interval, and the superscripts, TMB and SMB represent the TMB and the SMB processes, respectively. The migration velocities of the component i in the TMB can be quantified by the equilibrium theory. The resulting mass balances of the components are

$$\varepsilon_T\frac{\partial c_i}{\partial t} + (1-\varepsilon_T)\frac{\partial q_i}{\partial t} + (v_{L,j} - \varepsilon_P v_S)\frac{\partial c_i}{\partial z} - (1-\varepsilon_P)v_S\frac{\partial q_i}{\partial z} = 0$$
$$\text{s. t. } i \in \{1, \ldots, N\} \quad (2)$$

where c_i and q_i are, respectively, the liquid and solid phase concentrations of the component i, $v_{L,j}$ is the linear velocity of the liquid phase in zone j, and v_S is the linear velocity of the solid phase. The migration velocity of component i in zone j is

$$u_{i,j} = \frac{(v_{L,j} - \varepsilon_P v_S) - (1-\varepsilon_P)v_S(\mathcal{D}q_i/\mathcal{D}c_i)}{\varepsilon_T + (1-\varepsilon_T)(\mathcal{D}q_i/\mathcal{D}c_i)}$$
$$\text{s. t. } \frac{\mathcal{D}q_i}{\mathcal{D}c_i} = \frac{\partial q_i}{\partial c_1}\frac{dc_1}{dc_i} + \ldots + \frac{\partial q_i}{\partial c_N}\frac{dc_N}{dc_i} \quad (3)$$

The direction of the component migration is determined by the numerator, so that the component i migrates in the direction of the liquid phase flow in a specific zone j if $m_j > \mathcal{D}q_i/\mathcal{D}c_i$.

In the next sections, the theoretical background of the novel iterative short-cut design method for the conventional four-zone SMB process will be introduced. First, the approach is validated for binary mixtures. Afterward, the potential for multicomponent separations will be demonstrated for a quaternary mixture with Langmuir isotherms.

2.1. Solution of Equilibrium Theory. The TMB process is a continuous process which is operated in steady-states. The constant concentration feed mixture is continuously fed into the system. Therefore, it is equivalent to the Riemann problem of the hyperbolic conservation laws.[11] Let us consider the mass balance around the feed port as shown in Figure 2 (upper). In the steady-state, certain concentration plateaus are formed in zones 2 and 3. The concentrations can be the constant plateau concentrations (P in Figure 2) or the concentrations in the rarefaction waves (w^r in Figure 2). Let us call these concentrations the "attainable" concentrations of the corresponding zones. Therefore, the following mass balances can be formulated,

$$c_{i,F}Q_F + \tilde{c}_{i,2}(Q_2 - \varepsilon_P Q_S) - \tilde{c}_{i,3}(Q_3 - \varepsilon_P Q_S) = \tilde{q}_{i,2}(1-\varepsilon_P)Q_S - \tilde{q}_{i,3}(1-\varepsilon_P)Q_S \quad (4)$$

$$\tilde{c}_{i,2}m_2 - \tilde{c}_{i,3}m_3 + c_{i,F}(m_3 - m_2) = \tilde{q}_{i,2} - \tilde{q}_{i,3} \quad (5)$$

where $\tilde{c}_{i,j}$ is the attainable liquid phase concentration of component i in zone j, $c_{i,F}$ is the feed concentration of the component i, Q_F is the volumetric flow-rate of the feed stream, and $\tilde{q}_{i,j}$ is the attainable solid phase concentration of component i in zone j. At the fixed m-values of zones 2 and 3 (m_2 and m_3), the mass flux of the feed stream can be split to zones 2 and 3. When a mass split ratio φ is applied, eq 5 can be rewritten as

https://doi.org/10.1021/acs.iecr.1c00671
Ind. Eng. Chem. Res. 2021, 60, 10753−10763

$$\begin{cases} \tilde{q}_{i,2} = \tilde{c}_{i,2} m_2 + \varphi_i M_{i,F} \\ \tilde{q}_{i,3} = \tilde{c}_{i,3} m_3 - (1 - \varphi_i) M_{i,F} \end{cases}$$
$$\text{s. t. } M_{i,F} = c_{i,F}(m_3 - m_2) \tag{6}$$

where φ_i is the mass split ratio of component i toward the extract port. If $\varphi_1 = 1$ and $\varphi_1 = 0$ in a binary mixture system, the mixture is completely separated and the components 1 and 2 are collected pure at the extract and raffinate ports, respectively.

The equilibrium theory equations applied to describe the TMB process are a system of the hyperbolic partial differential equations (PDEs), cf. eq 2. It is well-known that the smooth solutions follow the fundamental differential equations (FDEs),[9]

$$\frac{\mathcal{D}q_1}{\mathcal{D}c_1} = \frac{\mathcal{D}q_2}{\mathcal{D}c_2} = \ldots = \frac{\mathcal{D}q_N}{\mathcal{D}c_N} \tag{7}$$

The FDEs provide the directions of the characteristic lines on the hodograph plane. If the characteristic lines intersect in the z-t plane, a discontinuous shock wave is formed and satisfies the conditions,

$$\frac{\Delta q_1}{\Delta c_1} = \frac{\Delta q_2}{\Delta c_2} = \ldots = \frac{\Delta q_N}{\Delta c_N} \tag{8}$$

where Δc and Δq are the differences of the liquid and solid phase concentrations across the shock wave, respectively. For example, the FDEs for the binary mixture can be expressed as

$$\frac{q_{1,1}dc_1 + q_{1,2}dc_2}{dc_1} = \frac{q_{2,1}dc_1 + q_{2,2}dc_2}{dc_2} \quad \text{s. t. } q_{i,j} = \frac{\partial q_i}{\partial c_j} \tag{9}$$

At a certain point (c_1^*, c_2^*) on the vector field of c_1 and c_2, there are two possible characteristic lines $\sigma_{2,1}^{\pm}$ with the slopes,

$$\zeta_{2,1}^{\pm} = \frac{dc_2}{dc_1} = \frac{q_{2,2} - q_{1,1} \pm \sqrt{(q_{1,1} - q_{2,2})^2 + 4q_{1,2}q_{2,1}}}{2q_{1,2}} \tag{10}$$

where $\zeta_{2,1}^{\pm}$ is the ratios of the concentration change of the component 2 with respect to the concentration change of the component 1.

In a ternary mixture system, the directions from the FDEs, which are the solutions of a cubic polynomial equation, can be still solved analytically. However, the FDEs do not have any analytical solution if there are more than three components in the feed. The general FDEs for the N-component system are,

$$\frac{q_{1,1}dc_1 + \ldots + q_{1,N}dc_N}{dc_1} = \ldots = \frac{q_{N,1}dc_1 + \ldots + q_{N,N}dc_N}{dc_N} \tag{11}$$

To solve the above given complex system of polynomial equations, many mathematical methods, such as the solution of an eigenvalue problem[17] or, more specific, for the case of Langmuir adsorption isotherms, the ω-transformation[11] were introduced.

2.2. Langmuir Isotherms for Multicomponent Systems. In liquid chromatography, the Langmuir isotherm equation is a well-proven isotherm model, which is widely used when the components retention times decrease as the concentrations increase. The concentrations of the mixture components are relatively low and the liquid phase media solvents are usually handled as an inert in liquid chromatography. Frequently, nonstoichiometric Langmuir isotherms with component-specific saturation capacities are applied to describe the competitive adsorption equilibria better.

$$q_i = \frac{q_{\max,i} K_i c_i}{1 + \sum_k K_k c_k} \quad \text{s. t. } i \in \{1, \ldots, N\} \tag{12}$$

For the purpose of this study, the isotherm derivatives are of essential relevance.

$$q_{i,j} = \begin{cases} \dfrac{q_{\max,i} K_i (1 - K_i c_i + \sum_k K_k c_k)}{(1 + \sum_k K_k c_k)^2}, & i = j \\ -\dfrac{q_{\max,i} K_i K_j c_i}{(1 + \sum_k K_k c_k)^2}, & i \neq j \end{cases} \tag{13}$$

where $q_{\max,i}$ is the maximum adsorption capacity of the component i and K_i is the equilibrium constant of the component i. The Henry constant H_i is equal to $q_{\max,i}K_i$. If the maximum adsorption capacities of all components are the same, the Langmuir isotherm is theoretically consistent and satisfies the ideal adsorbed solution theory.

When eqs 11 and 13 are combined, the FDEs can be written as

$$q_{\max,1} K_1 \frac{(1 + \sum_k K_k c_k)dc_1 - \sum_k K_k c_1 dc_k}{dc_1} = \ldots = q_{\max,N} K_N \frac{(1 + \sum_k K_k c_k)dc_N - \sum_k K_k c_N dc_k}{dc_N} \tag{14}$$

All independent variables, c_1 to c_N are of the first order and just linearly combined. Thus, the solution of the fundamental differential equations, eq 7 represents straight lines in the hodograph space of the fluid phase concentrations. Further, for Langmuir isotherms, the shock waves represented by eqs 8 are also straight lines and therefore coincide with the trajectories of eq 7. This alleviates the solution considerably.

2.3. Determination of Concentration Plateaus. In a Langmuir isotherm system, the selectivity, $\alpha_{i,j} = (c_j q_i)/(c_i q_j)$ is constant, so that the elution order of components is not changed. The internal concentration profiles of the TMB process can be divided into two sections. The desorption section is from the feed port to the desorbent port via the extract port (zones 1 and 2). In this section, the components are gradually desorbed due to fast liquid phase flow and move toward the liquid phase flow direction, so that the rarefaction waves are formed (e.g., w_1^r to w_4^r for a quaternary system in Figure 2 lower). In the adsorption section that is composed of zones 3 and 4, the components move toward the solid phase flow direction due to slow liquid phase flow. Therefore, the shock waves are formed in the adsorption section (e.g., w_1^s to w_4^s in Figure 2 lower). Let us assume that the liquid desorbent and solid adsorbent are completely regenerated in zones 4 and 1, respectively. On the base concentration plateau, P_0, the concentrations of all components are zero. Thus, two concentration points that represent the state of the adsorption and desorption sections can determine the hodograph lines by eq 14, and the concentration plateaus between two points can be revealed.

https://doi.org/10.1021/acs.iecr.1c00671
Ind. Eng. Chem. Res. 2021, 60, 10753−10763

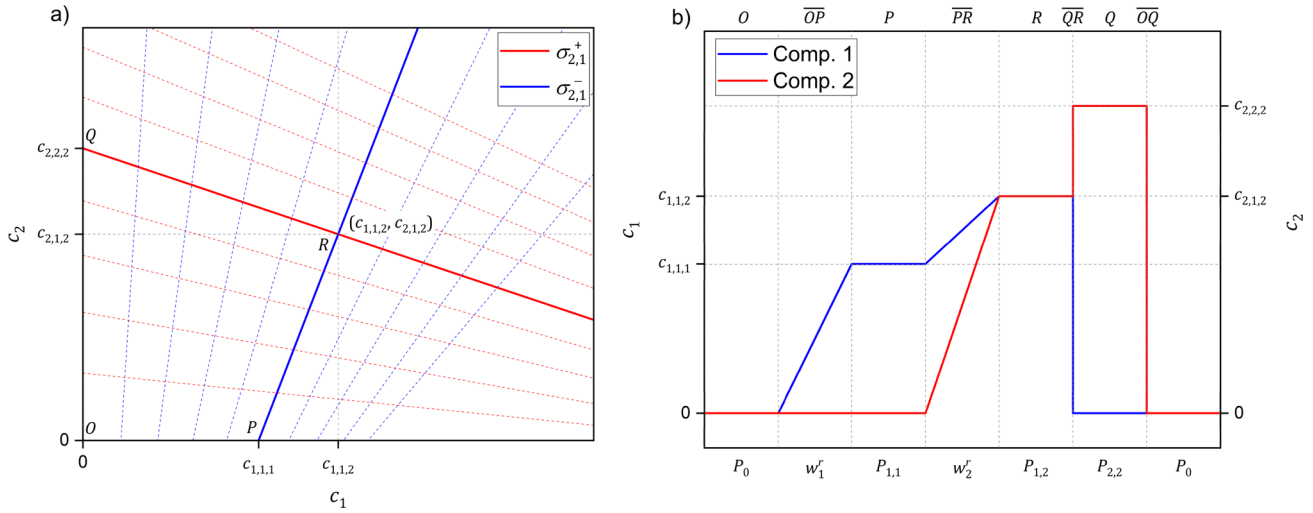

Figure 3. Hodograph of Riemann problem of TMB mass balance with binary Langmuir adsorption isotherms (a) and the corresponding concentration plateau chart (b).

In the adsorption section, the shock wave w_i^s is the connection between the neighboring plateaus, $P_{i,N}$ and $P_{i,1+N}$ (if $i = N$, P_0), and the migration velocity of the shock wave is determined by the partition ratio,

$$u_i^s = \frac{(v_L - \varepsilon_P v_S) - (1-\varepsilon_P)v_S(\Delta q_{i,i,N}/\Delta c_{i,i,N})}{\varepsilon_T + (1-\varepsilon_T)(\Delta q_{i,i,N}/\Delta c_{i,i,N})}$$

$$\text{s. t. } \frac{\Delta q_{i,i,N}}{\Delta c_{i,i,N}} = \frac{q_{i,i+1,N} - q_{i,i,N}}{c_{i,i+1,N} - c_{i,i,N}} = \frac{q_{i,i,N}}{c_{i,i,N}} \tag{15}$$

$$u_1^s < u_2^s < \ldots < u_N^s \Leftrightarrow \frac{q_{1,1,N}}{c_{1,1,N}} > \frac{q_{2,2,N}}{c_{2,2,N}} > \ldots > \frac{q_{N,N,N}}{c_{N,N,N}} \tag{16}$$

where u_i^s is the migration velocity of the shock wave w_i^s, and $c_{i,j,k}$ and $q_{i,j,k}$ are the liquid and solid phase concentrations of the component i on the plateau $P_{j,k}$, respectively. In the desorption section, the rarefaction wave w_i^r located between the neighboring plateaus, $P_{1,i-1}$ (if $i = 1$, P_0) and $P_{1,i}$ is distributed with different migration velocities of the front and rear ends. The migration velocities of both ends of the rarefaction wave are

$$u_i^{rf} = \frac{(v_L - \varepsilon_P v_S) - (1-\varepsilon_P)v_S(\mathcal{D}q_{i,1,i}/\mathcal{D}c_{i,1,i})}{\varepsilon_T + (1-\varepsilon_T)(\mathcal{D}q_{i,1,i}/\mathcal{D}c_{i,1,i})} \tag{17}$$

$$u_i^{rr} = \frac{(v_L - \varepsilon_P v_S) - (1-\varepsilon_P)v_S(\mathcal{D}q_{i,1,i-1}/\mathcal{D}c_{i,1,i-1})}{\varepsilon_T + (1-\varepsilon_T)(\mathcal{D}q_{i,1,i-1}/\mathcal{D}c_{i,1,i-1})} \tag{18}$$

$$u_1^{rr} < u_1^{rf} < u_2^{rr} < u_2^{rf} < \ldots < u_N^{rf}$$
$$\Leftrightarrow q_{M,1}K_1 > \frac{\mathcal{D}q_{1,1,1}}{\mathcal{D}c_{1,1,1}} > \frac{\mathcal{D}q_{2,1,2}}{\mathcal{D}c_{2,1,2}} > \ldots > \frac{\mathcal{D}q_{N,1,N}}{\mathcal{D}c_{N,1,N}} \tag{19}$$

where u_i^{rf} and u_i^{rr} are respectively the migration velocities of the front and rear ends of the rarefaction wave w_i^r.

2.4. Triangle Theory and Iterative Numerical Approach for Binary Separations. Let us recall the original triangle theory as introduced in ref 14. The essential operating conditions of the conventional four-zone SMB process are the design parameters, m_1 to m_4. The parameters for the regeneration zones 1 and 4 (m_1 and m_4) can be obtained from the Henry constant of the more-retained component (1) and the isotherm parameters of the less-retained component (2) combined with the product concentrations at the raffinate port, respectively.

$$m_1 \geq H_1 \tag{20}$$

$$\frac{-\varepsilon_P}{1-\varepsilon_P} \leq m_4 \leq \frac{1}{2}(D - \sqrt{D^2 - 4H_2m_3})$$
$$\text{s. t. } D = H_2 + m_3 + K_2c_{2,F}(m_3 - m_2) \tag{21}$$

The most important design parameters are the flow-rate ratios in the two separation zones, m_2 and m_3. The triangular separation region in the m_2−m_3 plane can be established analytically based on the coordiantes of four points.

$$\text{point } a\text{: } (H_1, H_1) \tag{22}$$

$$\text{point } b\text{: } (H_2, H_2) \tag{23}$$

$$\text{point } r\text{: } \left(\frac{\omega_G^2}{H_1}, \frac{\omega_G[\omega_F(H_1-\omega_G)(H_1-H_2) + H_2\omega_G(H_1-\omega_F)]}{H_1H_2(H_1-\omega_F)}\right) \tag{24}$$

$$\text{point } w\text{: } \left(\frac{H_2\omega_G}{H_1}, \frac{\omega_G[\omega_F(H_1-H_2) + H_2(H_B-\omega_F)]}{H_2(H_1-\omega_F)}\right) \tag{25}$$

The connecting lines $\overline{ab}$, $\overline{bw}$, and $\overline{rw}$ are straight. The connection $\overline{ar}$ is a curve.

$$\text{curve } \overline{ar}\text{: } m_3 = m_2 + \frac{(\sqrt{H_1} - \sqrt{m_2})^2}{K_1c_{1,F}} \tag{26}$$

Using the ω-transformation,[11] the four points mentioned above depend on two parameters ω_G and ω_F, which are the roots of the following quadratic equation determined by the feed concentrations and the equilibrium constants of the Langmuir isotherms ($\omega_G > \omega_F > 0$).

$$(1 + K_1c_{1,F} + K_2c_{2,F})\omega^2 - [H_1(1 + K_2c_{2,F}) + H_2(1 + K_1c_{1,F})]\omega + H_1H_2 = 0 \tag{27}$$

https://doi.org/10.1021/acs.iecr.1c00671
Ind. Eng. Chem. Res. 2021, 60, 10753−10763

The two ω parameters imply the plateau concentrations of the components (the points P and Q in Figure 3a) where the feed port plateau ($P_{1,2}$; the point R in Figure 3a) concentrations are $c_{1,F}$ and $c_{2,F}$. Therefore, the entire complete separation region can be drawn from the vertex point of the triangular region in the m_2−m_3 plane (point w in Figure 4).

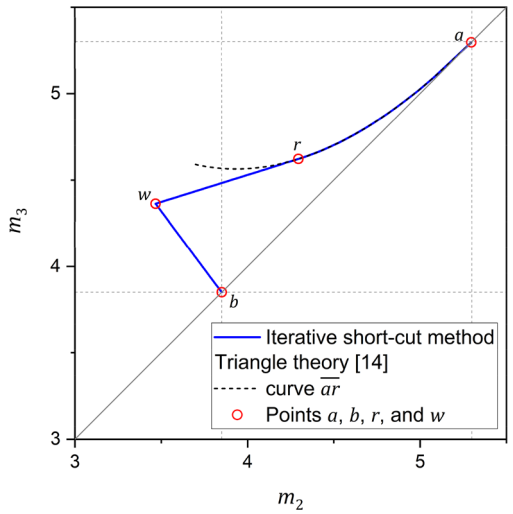

Figure 4. Comparisons of the separation regions obtained from the triangle theory and the iterative short-cut design method. Parameters used: $H_1 = 5.297$; $H_2 = 3.850$; $K_1 = 0.0321$ L/g; $K_2 = 0.0175$ L/g; $c_{1,F} = 5.0$ g/L; $c_{2,F} = 5.0$ g/L.

The triangle theory is a powerful tool to design the SMB process for complete separation. In some cases, the SMB processes are, however, intentionally operated at incomplete separation conditions for multicomponent separations to enhance process performances at the expense of product quality. Furthermore, it is difficult to identify the mass split ratios (φ_i) when the operating points are outside of the complete binary separation region.

In our iterative short-cut design method, the mass split ratios and the corresponding concentration plateau chart are numerically obtained by screening the exploitable minimum of m_2 and maximum of m_3 on a constant level from the diagonal line, that is, $m_3 - m_2 = \Delta m_{23} = \text{const}$. If the feed mass flux reaches to zero, that is, if $m_3 - m_2 \to 0$, $H_1 \le m_2 < m_3 \le H_2$. Starting points of the boundaries for pure extract and raffinate products are point a (H_1,H_1) and point b (H_2,H_2), respectively. At the first step, the difference between the m-values of zones 2 and 3 is increased by $\Delta m_{23}^{(1)}$. The initial points for the pure extract boundary screening can be obtained from the previous step result, $a_0^{(1)} = (m_{2,\min}^{(0)}, m_{2,\min}^{(0)} + \Delta m_{23}^{(1)})$ and $b_0^{(1)} = (m_{3,\max}^{(0)} - \Delta m_{23}^{(1)}, m_{3,\max}^{(0)})$ where $m_{2,\min}^{(0)} = H_1$ and $m_{3,\max}^{(0)} = H_2$. From the second step, the initial points $\{a_0^{(k)}, b_0^{(k)} | k \ge 2\}$ are obtained by extrapolation from the two previous steps. For example, the initial point $a_0^{(k)} = (2m_{2,\min}^{(k-1)} - m_{2,\min}^{(k-2)}, 2m_{2,\min}^{(k-1)} - m_{2,\min}^{(k-2)} + \Delta m_{23}^{(k)})$. If the boundaries for pure extract and raffinate products are crossed, it is not possible to get a feasible operating point for the complete separation. Therefore, the cross point of the two boundaries is the vertex point of the triangle separation region (the point w in Figure 4). With the given mass split ratios, φ_1 and φ_2, the mass balance equation, eq 6 can be solved, and the attainable concentrations in zones 2 and 3 ($\tilde{c}_2$ and $\tilde{c}_3$) are obtained. For well-posed m_2 and m_3, $\tilde{c}_2$ is on $\overline{OP}$ and $\overline{PR}$, and $\tilde{c}_3$ is on $\overline{QR}$ in Figure 3a. The entire hodograph trajectories (bold lines in Figure 3a) and the corresponding concentration plateau chart (Figure 3b) can be obtained from the FDEs (eq 10). The mass split ratios are numerically solved to minimize the differences of the attainable concentrations ($\tilde{c}_2$ and $\tilde{c}_3$) obtained from eq 6 and the hodograph chart. Within the range that satisfies $\varphi_1 = 1$ and $\varphi_1 = 0$, $m_{2,\min}^{(1)} = \max(\mathcal{D}q_{2,1,1}^{(1)}/\mathcal{D}c_{2,1,1}^{(1)})$ and $m_{3,\max}^{(1)} = \min(q_{1,1,2}^{(1)}/c_{2,1,1}^{(1)})$. These screening steps are repeated until $m_{2,\min}^{(k)} > m_{3,\max}^{(k)} - \Delta m_{23}^{(k)}$. Figure 4 shows the comparisons of the results provided by the explicit triangle theory (eqs 22−26) and the iterative short-cut design method. The points a, b, r, and w, and also curve $\overline{ar}$ were found to be in perfect agreement. The computational source codes of the iterative method are supplied in the Supporting Information.

This iterative method finds the points of the two boundaries of the complete separation regions by increasing Δm_{23}. Therefore, it consumes a lot of time and computational resources compared to the explicitly expressed triangle theory. However, it can be expanded for more sophisticated adsorption isotherms and multicomponent systems for which there is no explicit solution to describe the complete separation region of the conventional four-zone SMB processes.

2.5. Short-Cut Design for Multicomponent System.

The iterative short-cut design method described in section 2.4 can be extended to more complex mixtures containing N components. Let us presume that the components 1 to L elute at the extract port and the components M to N elute at the raffinate port ($H_1 > H_2 > \ldots > H_N$). If the component M is next to the component L ($L + 1 = M$), it is the complete pseudo-binary separation, that is, $\varphi_1 = \ldots = \varphi_L = 1$ and $\varphi_M = \ldots = \varphi_N = 0$. Since only two points in the concentration plateau chart that correspond to the attainable concentrations of zones 2 and 3 are revealed, the plateaus and waves between these two points constricted into the feed port. The constricted plateaus, $P_{1,L+1}$ to $P_{M-1,N}$ can be revealed by solving the following system of linear equations.

$$P_{1,L+1}: \left(\left.\frac{\mathrm{d}c_{L+1}}{\mathrm{d}c_1}\right|_{c=\tilde{c}_D}\right)(c_{1,1,L+1} - \tilde{c}_{1,D}) = \left(\left.\frac{\mathrm{d}c_{L+1}}{\mathrm{d}c_2}\right|_{c=\tilde{c}_D}\right)(c_{2,1,L+1} - \tilde{c}_{2,D}) = \ldots = c_{L+1,1,L+1}$$

$$\vdots$$

$$P_{1,N}: \left(\left.\frac{\mathrm{d}c_N}{\mathrm{d}c_1}\right|_{c=c_{1,N-1}}\right)(c_{1,1,N} - c_{1,1,N-1}) = \left(\left.\frac{\mathrm{d}c_N}{\mathrm{d}c_2}\right|_{c=c_{1,N-1}}\right)(c_{2,1,N} - c_{2,1,N-1}) = \ldots = c_{N,1,N}$$

https://doi.org/10.1021/acs.iecr.1c00671
Ind. Eng. Chem. Res. 2021, 60, 10753−10763

$$P_{1,N}\text{: } c_{1,1,N} = \left(\left.\frac{dc_1}{dc_2}\right|_{c=c_{2,N}}\right)(c_{2,1,N} - c_{2,2,N}) = \ldots = \left(\left.\frac{dc_1}{dc_N}\right|_{c=c_{2,N}}\right)(c_{N,1,N} - c_{N,2,N})$$

$$\vdots$$

$$P_{M-1,N}\text{: } c_{M-1,M-1,N} = \left(\left.\frac{dc_{M-1}}{dc_M}\right|_{c=\tilde{c}_A}\right)(c_{M,M-1,N} - \tilde{c}_{M,A}) = \ldots = \left(\left.\frac{dc_{M-1}}{dc_N}\right|_{c=\tilde{c}_A}\right)(c_{N,M-1,N} - \tilde{c}_{N,A}) \quad (28)$$

where $\boldsymbol{c}_{j,k}$ is the concentration vector on the plateau $P_{j,k}$, and $\tilde{\boldsymbol{c}}_A$ and $\tilde{\boldsymbol{c}}_D$ are the attainable concentration vectors of the adsorption (A) and desorption (D) sections, respectively. $\tilde{\boldsymbol{c}}_A$ and $\tilde{\boldsymbol{c}}_D$ should not contain any nonzero common element, and $\tilde{\boldsymbol{c}}_A = \tilde{\boldsymbol{c}}_3$ and $\tilde{\boldsymbol{c}}_D = \tilde{\boldsymbol{c}}_2$. The slopes dc_i/dc_j can be obtained from eq 14. Therefore, there exist only one solution.

In the incomplete pseudo-binary separations where $L \geq M$, $0 < \varphi_M, \ldots, \varphi_L < 1$. This means that $\tilde{\boldsymbol{c}}_2$ and $\tilde{\boldsymbol{c}}_3$ contain at least one nonzero common element. Therefore, the attainable concentration vector of the desorption section, $\tilde{\boldsymbol{c}}_D$ should be obtained by

$$P_{1,L-1}\text{: } \left(\left.\frac{dc_L}{dc_1}\right|_{c=\tilde{c}_2}\right)(c_{1,1,L-1} - \tilde{c}_{1,2}) = \left(\left.\frac{dc_L}{dc_2}\right|_{c=\tilde{c}_2}\right)(c_{2,1,L-1} - \tilde{c}_{2,2}) = \ldots = -\tilde{c}_{L,2}$$

$$\vdots$$

$$P_{1,M-1}\text{: } \left(\left.\frac{dc_M}{dc_1}\right|_{c=c_{1,M}}\right)(\tilde{c}_{1,D} - c_{1,1,M}) = \left(\left.\frac{dc_M}{dc_2}\right|_{c=c_{1,M}}\right)(\tilde{c}_{2,D} - c_{2,1,M}) = \ldots = -c_{M,1,M} \quad (29)$$

To assess if the mass split ratios are correctly assigned, the concentration vectors obtained from the mass balance, eq 6 and the migration direction determined by the hodograph solution should satisfy the following essential conditions. For zone 2, $\tilde{\boldsymbol{c}}_2$ should be on the rarefaction wave, w_L^r or on the plateau $P_{1,L}$. If $\tilde{\boldsymbol{c}}_2$ is on the rarefaction wave, w_L^r,

$$\frac{\mathcal{D}q_{L,1,L}}{\mathcal{D}c_{L,1,L}} < m_2 \leq \frac{\mathcal{D}q_{L,1,L-1}}{\mathcal{D}c_{L,1,L-1}} \quad (30)$$

or

$$\frac{\mathcal{D}q_{L+1,1,L}}{\mathcal{D}c_{L+1,1,L}} \leq m_2 \leq \frac{\mathcal{D}q_{L,1,L}}{\mathcal{D}c_{L,1,L}} \quad (31)$$

if $\tilde{\boldsymbol{c}}_2$ is on the plateau $P_{1,L}$. Therefore,

$$\frac{\mathcal{D}q_{L+1,1,L}}{\mathcal{D}c_{L+1,1,L}} \leq m_2 \leq \frac{\mathcal{D}q_{L,1,L-1}}{\mathcal{D}c_{L,1,L-1}} \quad (32)$$

For zone 3, $\tilde{\boldsymbol{c}}_3$ is always on the plateau $P_{M,N}$, and

$$\frac{q_{M,M,N}}{c_{M,M,N}} \leq m_3 \leq \frac{q_{M-1,M-1,N}}{c_{M-1,M-1,N}} \quad (33)$$

The conditions, eqs 32 and 33, are also the necessary conditions for the successful separation. Therefore, the m-values of zones 2 and 3 should satisfy the above inequality conditions to achieve designated separations. These inequality conditions provide different separation ranges of m_2 and m_3 with respect to the reduced feed mass flux defined as $M_{i,F} = c_{i,F}(m_3 - m_2)$. Therefore, the separation region on the m_2–m_3 plane should be screened from the diagonal line ($m_3 = m_2$) up to $\frac{\mathcal{D}q_{L+1,1,L}}{\mathcal{D}c_{L+1,1,L}} = \frac{q_{M-1,M-1,N}}{c_{M-1,M-1,N}}$ by increasing Δm_{23} ($= m_3 - m_2$). Here, component 1 is slowest, and the partition coefficient reaches H_1 as the concentration is diluted, so that the m-value of zone 1 should be higher than the Henry constant of component 1 for the complete regeneration of adsorbent, eq 20. The component concentrations at the raffinate port can be obtained from the overall mass balance and are the inlet concentrations of zone 4.

$$c_{i,R} = \frac{(1 - \varphi_i)M_{i,F}}{m_3 - m_4} \quad (34)$$

The height of the fastest plateau in the adsorption section can be determined by

$$P_{M+1,N}\text{: } -\tilde{c}_{M,A} = \left(\left.\frac{dc_M}{dc_{M+1}}\right|_{c=\tilde{c}_R}\right)(c_{M+1,M+1,N} - \tilde{c}_{M+1,A}) = \ldots = \left(\left.\frac{dc_M}{dc_N}\right|_{c=\tilde{c}_R}\right)(c_{N,M+1,N} - \tilde{c}_{N,A})$$

$$\vdots$$

$$P_{N,N}\text{: } -c_{N-1,N-1,N} = \left(\left.\frac{dc_{N-1}}{dc_N}\right|_{c=c_{N-1,N}}\right)(c_{N,N,N} - c_{N,N-1,N}) \quad (35)$$

Therefore, the m-value of zone 4 should satisfy the following condition to generate desorbent completely.

$$-\frac{\varepsilon_p}{1 - \varepsilon_p} \leq m_4 \leq \frac{q_{\max,N}K_N}{1 + K_N c_{N,N,N}} \quad (36)$$

The maximum m-value of zone 4, $m_{4,\max}$ assuring complete regeneration of the desorbent can be obtained by iteratively solving the implicit equation,

$$m_4 = \frac{q_{\max,N}K_N}{1 + K_N c_{N,N,N}} \quad \text{s. t. } c_{N,N,N} = f(m_2, m_3, m_4) \quad (37)$$

3. RESULTS AND DISCUSSION

3.1. Model System—Quaternary Mixture with Langmuir Isotherms. For Langmuir adsorption isotherms, there exist analytical solutions of the equilibrium theory up to ternary feed mixtures,[20] so that, a quaternary mixture system was

https://doi.org/10.1021/acs.iecr.1c00671
Ind. Eng. Chem. Res. 2021, 60, 10753−10763

chosen as an example to demonstrate the concept and the potential of the iterative numerical short-cut design method. The isotherm parameters are given in Table 1. The parameters

Table 1. Langmuir Isotherm Parameters and Henry Constants of the Quaternary Mixture Considered as the Model Mixture

components	q_{max} [g/L]	K [L/g]	H [-][a]
S_1	220	0.0321	7.062
S_2[b]	165	0.0321	5.297
S_3[b]	220	0.0175	3.850
S_4	165	0.0175	2.888

[a]Henry constant = $q_M K$. [b]Parameters from eq 14.

of the two components 2 and 3 were obtained from,[14] and the parameters of the most- and least-retained components, 1 and 4 were generated accordingly from the parameters of the components 2 and 3. Two pair of components, 1−2 and 3−4, have the same equilibrium constants, but the maximum adsorption capacities of the components 1 and 2 are the same as the components 3 and 4, respectively.

To obtain the separation region in the m_2−m_3 plane, Microsoft Excel (Microsoft Inc., U.S.A., Ver. 2019) was used with a built-in nonlinear solver and Marquardt method. The separation regions were screened with the fixed interval, $\Delta m_{23} = 0.01(H_1 - H_4) = 0.042$. The tolerance was set to 0.001 for the iterative numerical method. To validate the separation region calculated by the iterative short-cut design method, numerical simulations with the TMB process model were carried out with the system parameters listed in Table 2. For this Aspen Chromatography (AspenTech Inc. U.S.A, Ver. 8.8) was used.

Table 2. System Parameters for the TMB Simulation

parameters	values
feed concentrations	5.0 for each
c_F [g/l]	component
column	10
length [cm]	1.0
i.d. [cm]	0.42
void fraction [-]	1.0×10^{-3}
D_e [cm^2/min]	1000
k_{eff} [1/min]	
configuration[a]	
cases 1 to 5	1-1-1-1
cases 3 and 4	1-9-1-1
numerical method	
PDE solver	FDM with UD scheme
no. of nodes	200 per column
integrator	Explicit Euler

[a]Number of columns in {Zone 1}-{Zone 2}-{Zone 3}-{Zone 4}.

3.2. Complete Separation Region in the m_2−m_3 Plane for a Quaternary Feed Mixture. So far, it has not been discussed in detail how to obtain the separation region of the conventional four-zone SMB process for performing pseudo-binary separations of a multicomponent feed mixture. In practical aspects, one approximate design method of the four-zone SMB process for multicomponent system is simplifying it to binary mixture system with two key-components. For example, the separation region of the binary components 1 and 3 (1/3 in Figure 5a) is obtained if the key components are 1 and 3. In this case, the intermediate component 2 splits into the extract and raffinate ports, and the least-retained component 4 elutes at the raffinate port. The binary short-cut method underestimates the nonlinear adsorption behavior of the components omitting the existence of the components 2 and 4. Therefore, additional time and resources would be consumed in a subsequent detailed process design.

Figure 5 compares the separation regions obtained by approximated binary short-cut design method and the iterative multicomponent short-cut design method introduced in this work. As mentioned above, the approximated binary short-cut design method provides a large separation region compared to the iterative multicomponent short-cut design method. In the quaternary separation region (Figure 5b), the subseparation regions (β_1 to β_6) were clearly partitioned. In the subseparation regions β_1 to β_3, the quaternary mixture could be clearly separated into two solute groups, so that the mass split ratios of the components are 1 or 0. However, the quaternary mixture could not be separated into two groups in other subseparation regions, β_4 to β_6. In β_6, the most- and the least-retained components, 1 and 4, could be completely isolated at the extract and the raffinate ports, respectively ($\varphi_1 = 1$ and $\varphi_4 = 0$), but the other components are split into the extract and the raffinate ports ($0 < \varphi_2, \varphi_3 < 1$). The boundaries of subseparation regions indicate the minimum m-value of zone 2 to prevent the component i from eluting to the extract port ($m^i_{2,min}$) and the maximum m-value of zone 3 to prevent the component i from eluting to the raffinate port ($m^i_{3,max}$). The slopes of $m_{2,min}$ and $m_{3,max}$ changed where they intersect each other. For example, the slope of $m^4_{2,min}$ significantly ramped, and the slope of $m^4_{2,max}$ flattened where it entered the higher subseparation region ($\beta_3 \rightarrow \beta_5 \rightarrow \beta_6$ in Figure 3b solid blue line and $\beta_1 \rightarrow \beta_4 \rightarrow \beta_6$ in Figure 5b solid red line).

For Langmuir isotherms, the retention behavior of the components tends to become nonlinear as the concentrations increase. To further investigate the changes of the complete quaternary separation regions due to the isotherm nonlinearity, the component concentrations in the feed were changed from 1 g/L to 10 g/L for all components. For 1 g/L in Figure 6a, the boundaries for m_2 are almost vertical and the boundaries for m_3 are almost horizontal. This means that the separation regions are close to those of the linear isotherms as the feed concentration decreases, that is, the effect of the isotherm nonlinearity weakens. As the feed concentrations increased to 5 g/L and 10 g/L, the separation regions tend to lie close to the diagonal line (Figure 6b,c).

To validate the subseparation regions, five operating conditions were chosen at the 5 g/L of feed concentration condition (red circles on Figure 6b). The m-values of zones 1 and 4 were determined with a 20% safety margin, $m_1 = 1.2 \times H_1$ and $m_4 = 0.8 \times m_{4,max}$. The operating conditions of cases 1 to 4 were close to the cross point of two boundaries, $m^3_{2,min}$ and $m^2_{2,max}$, and located in different subseparation regions (β_2, β_4, β_6, and β_5 in consecutive order). The operating conditions of case 5 were close to the vertex of the separation region, which indicates the optimal operating conditions with high productivity. As shown in Table 3, the mass split ratios calculated by the iterative short-cut design method and obtained from the TMB process simulations were in good agreement, and the mass split ratios satisfied the subseparation regions.

The internal concentration profiles obtained from the TMB process simulation and the plateau concentrations calculated by

https://doi.org/10.1021/acs.iecr.1c00671
Ind. Eng. Chem. Res. 2021, 60, 10753−10763

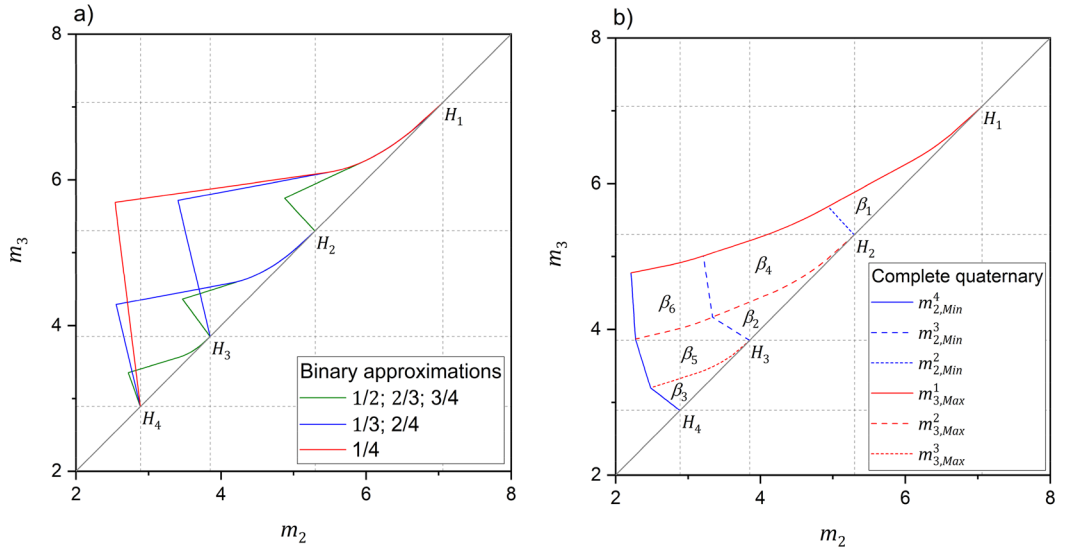

Figure 5. Approximated separation regions by binary short-cut design method (a) and complete quaternary separation regions by iterative short-cut design method (b). β_1, region for the separation of components 1 and 2−4; β_2, region for the separation of components 1−2 and 3−4; β_3, region for the separation of components 1−3 and 4; β_4, region for the separation of components 1−2 and 2−4; β_5, region for the separation of components 1−3 and 3−4; β_6, region for the separation of components 1−3 and 2−4.

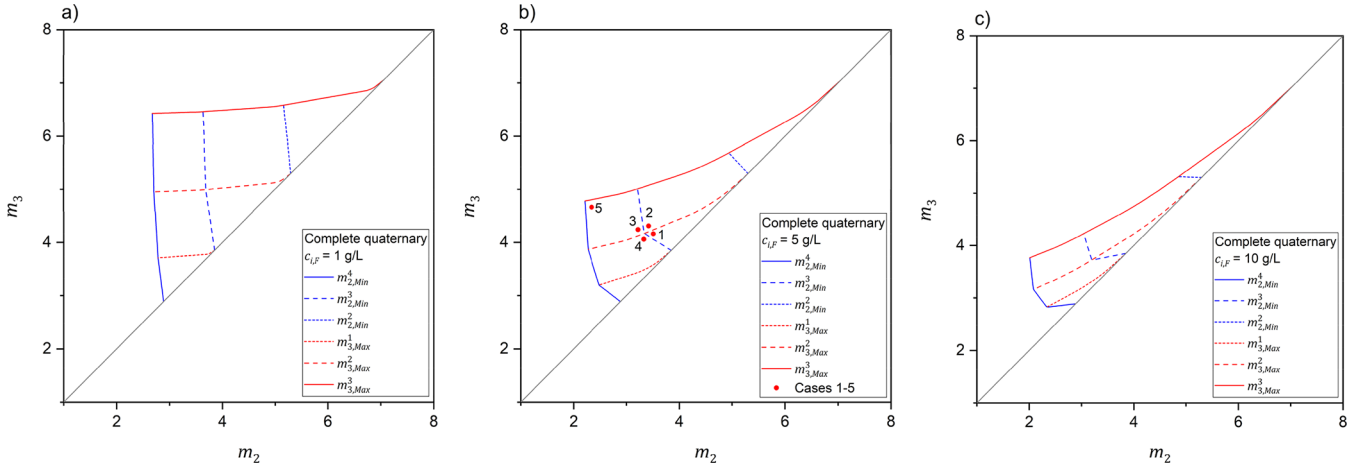

Figure 6. Changes of the complete quaternary separation regions by the feed concentrations: (a) $c_{i,F}$ = 1 g/L; (b) $c_{i,F}$ = 5 g/L; (c) $c_{i,F}$ = 10 g/L; red circles, selected operating points for the TMB process simulation, cf., Table 3.

Table 3. Operating Conditions and Mass Split Ratios Calculated by the Iterative Short-Cut Design Method and the TMB Process Simulation

	operating conditions				mass split ratio, φ_i [%][a]			
	m_1	M_2	M_3	M_4	A	B	C	D
case 1	8.47	3.51	4.16	2.21	100 (100)	100 (99.8)	0.00 (0.00)	0.00 (0.00)
case 2	8.47	3.42	4.31	2.19	100 (100)	84.7 (84.5)	0.00 (0.00)	0.00 (0.00)
case 3	8.47	3.22	4.24	2.16	100 (100)	85.4 (85.2)	0.51 (0.51)	0.00 (0.00)
case 4	8.47	3.33	4.06	2.19	100 (100)	100 (99.8)	0.75 (0.74)	0.00 (0.00)
case 5	8.47	2.34	4.66	2.05	100 (99.9)	57.7 (57.5)	17.0 (17.0)	0.00 (0.00)

[a]Values in the parentheses: mass split ratio obtained from the TMB simulation with 1-1-1-1 configurations for cases 1, 2, and 5, and 1-9-1-1 configurations for cases 3 and 4.

the iterative short-cut design method are compared in Figure 7. In case 1, the quaternary mixture is completely separated into two groups. The components 1 and 2 elute at the extract port and the components 3 and 4 elute at the raffinate port. To collect the components 1 and 2 in the extract port, m_2 (= 3.51) should be smaller than $\mathcal{D}q_{2,1,1}/\mathcal{D}c_{2,1,1}$ (= 5.16) and greater than $\mathcal{D}q_{3,1,2}/\mathcal{D}c_{3,1,2}$ (= 3.42), cf., Figure 7c and eq 32. On the other hand, the m-value of zone 2 in case 3 (m_2 = 3.22) was smaller than $\mathcal{D}q_{3,1,2}/\mathcal{D}c_{3,1,2}$ (= 3.32), so that some amount of component 3 elutes at the extract port together with components 1 and 2. Since m_2 led to a value which belongs to a rarefaction wave, w^3_r

https://doi.org/10.1021/acs.iecr.1c00671
Ind. Eng. Chem. Res. 2021, 60, 10753−10763

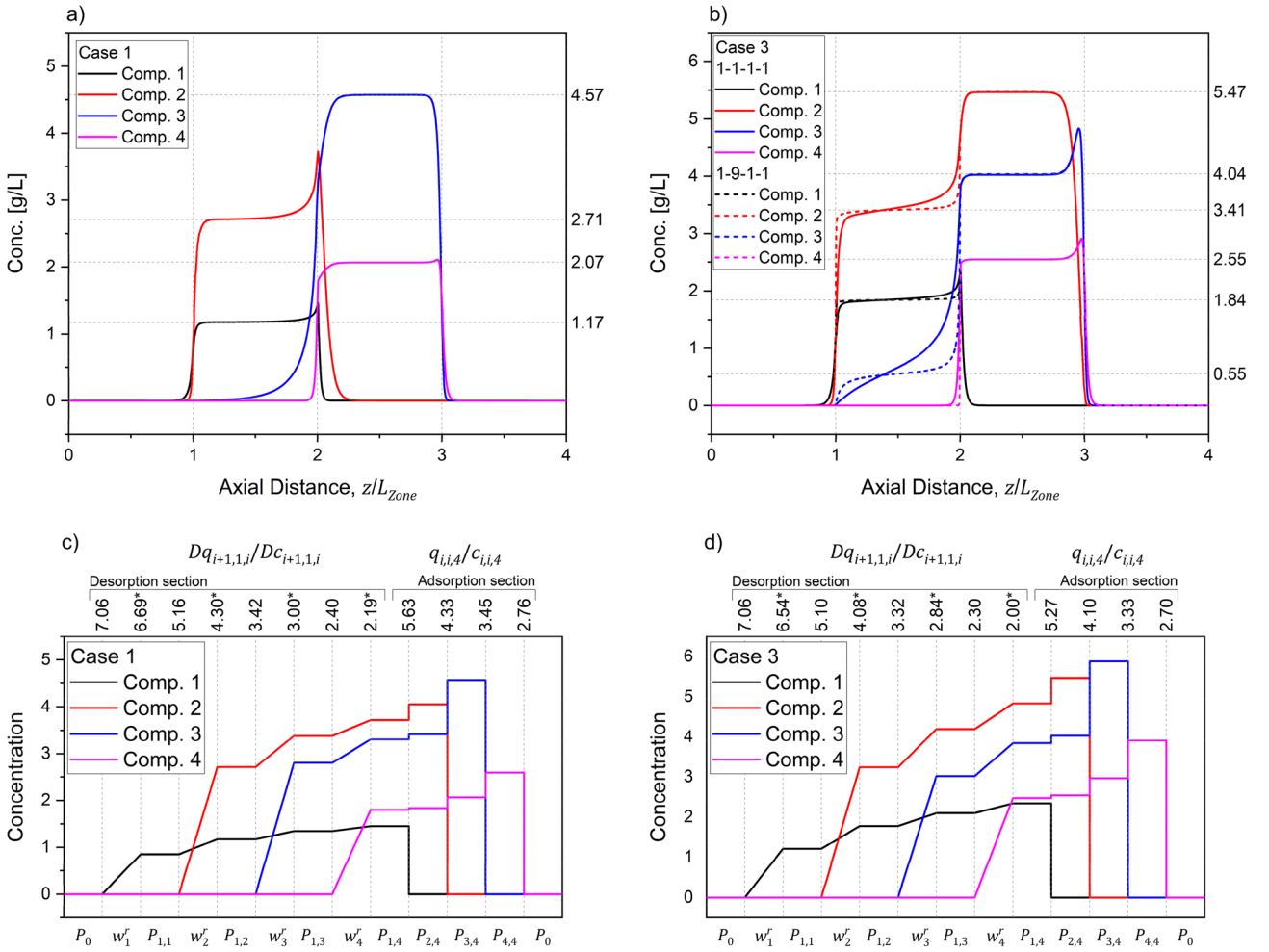

Figure 7. Comparisons of the internal concentration profiles as a result of simulating the TMB process (a and b) and the plateau chart obtained from the iterative short-cut design method (c and d). (a, c) Case 1; (b, d) case 3; cf., Table 3. The asterisk (∗) denotes $\mathcal{D}q_{i,1,i}/\mathcal{D}c_{i,1,i}$.

(= [2.84, 3.32], Figure 7d), the TMB process simulation that used a 1-1-1-1 column configuration could not achieve clear concentration plateaus in zone 2. For better resolution, a 1-9-1-1 configuration with eight more columns in zone 2 was applied, and clear plateaus were observed in zone 2 (dotted lines in Figure 7b). The horizontal reference lines and the values on the right-hand side in Figure 7a,b indicated the plateau concentrations obtained from the iterative short-cut design method, and they were met.

4. CONCLUSION

An iterative short-cut design method that extends the well-known triangle theory to treat multicomponent systems was introduced and demonstrated for a quaternary mixture characterized by nonstoichiometric Langmuir isotherms. The applicability of the obtained design parameters was successfully validated by numerical TMB simulations. The mass split ratios, which describe the split of the feed mass toward zones 2 and 3, play an important role in practice, for example, for the fractionation of complex mixtures (as an incomplete quaternary separation considered in this work) and for the design of modified SMB processes for center-cut separations.[21] As described in sections 2.3 and 2.4, the iterative short-cut design method directly solves the FDEs, eq 7, numerically. Therefore, we believe that this method has considerable potential for the efficient design of continuous multicolumn adsorptive separation processes.

■ ASSOCIATED CONTENT

Supporting Information

The Supporting Information is available free of charge at https://pubs.acs.org/doi/10.1021/acs.iecr.1c00671.

An example of the iterative method for a quaternary mixture separation (ZIP)

■ AUTHOR INFORMATION

Corresponding Author

Ju Weon Lee − *Institute for Automation Engineering, Otto von Guericke University, Magdeburg 39106, Germany; Max Planck Institute for Dynamics of Complex, Magdeburg 39106, Germany;* orcid.org/0000-0002-1459-1038; Phone: +49 391 6110392; Email: lee@mpi-magdeburg.mpg.de

Authors

Achim Kienle − *Institute for Automation Engineering, Otto von Guericke University, Magdeburg 39106, Germany; Max Planck Institute for Dynamics of Complex, Magdeburg 39106, Germany*

Andreas Seidel-Morgenstern − *Max Planck Institute for Dynamics of Complex, Magdeburg 39106, Germany; Institute*

of Chemical Engineering, Otto von Guericke University, Magdeburg 39106, Germany; orcid.org/0000-0001-7658-7643

Complete contact information is available at: https://pubs.acs.org/10.1021/acs.iecr.1c00671

Notes

The authors declare no competing financial interest.

■ ACKNOWLEDGMENTS

This research was funded by the Deutsche Forschungsgemeinschaft (DFG, German Research Foundation) Grant LE 4481/2-1, project no. 441831362.

■ DEDICATION

The authors dedicate this paper to Guiseppe Storti to acknowledge his eminent contributions to design SMB processes.

■ REFERENCES

(1) Kaspereit, M.; Schmidt-Traub, H. Process concepts. In *Preparative chromatography*, 3rd ed.; Schmidt-Traub, H., Schulte, M., Seidel-Morgenstern, A., Eds.; Wiley-VCH: Weinheim, 2020; Chapter 5.

(2) Broughton, C. B.; Gerhold, C. G. Continuous sorption process employing fixed bed of sorbent and moving inlets and outlets. U.S. Patent 2,985,589, 1961.

(3) Johnson, J. A.; Kabza, R. G. Sorbex: Industrial-scale adsorptive separation. In *Preparative and production scale chromatography*; Ganetsos, G., Barker, P. E., Eds.; Marcel Dekker: New York, 1993; Chapter 12.

(4) Bubnik, Z.; Pour, V.; Gruberova, A.; Starhova, H.; Hinkova, A.; Kadlec, P. Application of continuous chromatographic separation in sugar processing. *J. Food Eng.* **2004**, *61*, 509.

(5) Negawa, M.; Shoji, F. Optical resolution by simulated moving-bed adsorption technology. *J. Chromatogr.* **1992**, *590*, 113.

(6) Rajendran, A.; Paredes, G.; Mazzotti, M. Simulated moving bed chromatography for the separation of enantiomers. *J. Chromatogr. A* **2009**, *1216*, 709.

(7) Kawajiri, Y. Model-based optimization strategies for chromatographic processes: a review. *Adsorption* **2021**, *27*, 1.

(8) Rodrigues, A. E.; Pereira, C.; Menceva, M.; Pais, L. S.; Ribeiro, A. M.; Ribeiro, A.; Silva, M.; Garca, N.; Santos, J. C. *Simulated moving bed technology: Principles, design, and process applications*; Butterworth-Heinemann: Oxford, 2015.

(9) Rhee, H. K.; Aris, R.; Amundson, N. R. On the theory of multicomponent chromatography. *Philos. Trans. Royal Soc. A* **1970**, *267*, 419.

(10) Rhee, H. K.; Aris, R.; Amundson, N. R. *First-order Partial Differential Equations, Vol. 1: Theory and applications of single equations*; Prentice-Hall: Englewood Cliffs, 1986.

(11) Rhee, H. K.; Aris, R.; Amundson, N. R. *First-order Partial Differential Equations, Vol. 2: Theory and applications of hyperbolic systems of quasilinear equations*; Prentice-Hall: Englewood Cliffs, 1989.

(12) Mazzotti, M.; Rajendran, A. Equilibrium theory–based analysis of nonlinear waves in separation processes. *Annu. Rev. Chem. Biomol. Eng.* **2013**, *4*, 119.

(13) Storti, G.; Mazzotti, M.; Morbidelli, M.; Carra, S. Robust design of binary countercurrent separation processes. *AIChE J.* **1993**, *39*, 471.

(14) Mazzotti, M.; Storti, G.; Morbidelli, M. Optimal operation of simulated moving bed units for nonlinear chromatographic separations. *J. Chromatogr. A* **1997**, *769*, 3.

(15) Migliorini, C.; Mazzotti, M.; Morbidelli, M. Robust design of countercurrent adsorption separation processes: 5. Nonconstant selectivity. *AIChE J.* **2000**, *46*, 1384.

(16) Mazzotti, M. Design of simulated moving bed separations: generalized Langmuir isotherm. *Ind. Eng. Chem. Res.* **2006**, *45*, 6311.

(17) Fechtner, M.; Kienle, A. Efficient simulation and equilibrium theory for adsorption processes with implicit adsorption isotherm - Mass action equilibria. *Chem. Eng. Sci.* **2017**, *171*, 471.

(18) Fechtner, M.; Kienle, A. Rational design of ion exchange simulated moving bed processes. *Comput.-Aided Chem. Eng.* **2020**, *48*, 733.

(19) Myers, A. L.; Prausnitz, J. M. Thermodynamics of mixed-gas adsorption. *AIChE J.* **1965**, *11*, 121.

(20) Lee, J. W.; Wankat, P. C. Optimized design of recycle chromatography to isolate intermediate retained solutes in ternary mixtures: Langmuir isotherm systems. *J. Chromatogr. A* **2009**, *1216*, 6946.

(21) Lee, J. W. Expanding simulated moving bed chromatography into ternary separations in analogy to dividing wall column distillation. *Ind. Eng. Chem. Res.* **2020**, *59*, 9619.